Received: 1 October 2018 | Revised: 14 March 2019 | Accepted: 17 March 2019

DOI: 10.1111/gcb.14625

PRIMARY RESEARCH ARTICLE

Global Change Biology WILEY

Spatial resilience of the Great Barrier Reef under cumulative disturbance impacts

Camille Mellin[1,2] | Samuel Matthews[1,3] | Kenneth R.N. Anthony[1,4] | Stuart C. Brown[2] | M. Julian Caley[5,6] | Kerryn A. Johns[1] | Kate Osborne[1] | Marjetta Puotinen[7] | Angus Thompson[1] | Nicholas H. Wolff[8,9] | Damien A. Fordham[2,10] | M. Aaron MacNeil[1,11]

[1]Australian Institute of Marine Science, Townsville MC, Townsville, Qld, Australia

[2]The Environment Institute and School of Biological Sciences, University of Adelaide, Adelaide, South Australia, Australia

[3]Australian Research Council Centre of Excellence for Coral Reef Studies, James Cook University, Townsville, Qld, Australia

[4]School of Biological Sciences, The University of Queensland, St Lucia, Qld, Australia

[5]School of Mathematical Sciences, Queensland University of Technology, Brisbane, Qld, Australia

[6]Australian Research Council Centre of Excellence for Mathematical and Statistical Frontiers, Brisbane, Qld, Australia

[7]Australian Institute of Marine Science, Indian Ocean Marine Research Centre, University of Western Australia, Crawley, WA, Australia

[8]Global Science, The Nature Conservancy, Brunswick, Maine

[9]Marine Spatial Ecology Lab, School of Biological Sciences, The University of Queensland, St Lucia, Qld, Australia

[10]Center for Macroecology, Evolution, and Climate, Natural History Museum of Denmark, University of Copenhagen, Copenhagen, Denmark

[11]Department of Biology, Dalhousie University, Halifax, NS, Canada

Correspondence
Camille Mellin, The Environment Institute and School of Biological Sciences, University of Adelaide, Adelaide, South Australia, Australia.
Email: camille.mellin@adelaide.edu.au

Funding information
Australian Research Council, Grant/Award Number: DE140100701

Abstract

In the face of increasing cumulative effects from human and natural disturbances, sustaining coral reefs will require a deeper understanding of the drivers of coral resilience in space and time. Here we develop a high-resolution, spatially explicit model of coral dynamics on Australia's Great Barrier Reef (GBR). Our model accounts for biological, ecological and environmental processes, as well as spatial variation in water quality and the cumulative effects of coral diseases, bleaching, outbreaks of crown-of-thorns starfish (*Acanthaster* cf. *solaris*), and tropical cyclones. Our projections reconstruct coral cover trajectories between 1996 and 2017 over a total reef area of 14,780 km^2, predicting a mean annual coral loss of −0.67%/year mostly due to the impact of cyclones, followed by starfish outbreaks and coral bleaching. Coral growth rate was the highest for outer shelf coral communities characterized by digitate and tabulate *Acropora* spp. and exposed to low seasonal variations in salinity and sea surface temperature, and the lowest for inner-shelf communities exposed to reduced water quality. We show that coral resilience (defined as the net effect of resistance and recovery following disturbance) was negatively related to the frequency of river plume conditions, and to reef accessibility to a lesser extent. Surprisingly, reef resilience was substantially lower within no-take marine protected areas, however this difference was mostly driven by the effect of water quality. Our model provides a new validated, spatially explicit platform for identifying the reefs that face the greatest risk of biodiversity loss, and those that have the highest chances to persist under increasing disturbance regimes.

KEYWORDS

Acanthaster, bleaching, coral reefs, crown-of-thorns, cyclones, water quality

1 | INTRODUCTION

Natural ecosystems are facing unprecedented and accelerating degradation (Ceballos et al., 2015), as exemplified by increasing rates of losses of coral reef biodiversity in the 21st century due to anthropogenic and natural stresses and their interactions (Hughes et al., 2017; Knowlton, 2001). Coral reefs are among the most species-rich ecosystems globally (Caley, Fisher, & Mengersen, 2014), hosting hundreds of thousands of species (Fisher et al., 2015) and providing important ecosystem services (Costanza et al., 2014). Consequently, the potential impacts of anthropogenic stresses are especially high for coral reef ecosystems.

The resilience of an ecosystem can be defined as its capacity to absorb the impact of a disturbance and return to its initial state (Folke et al., 2004; Hughes et al., 2003; Hughes, NaJ, Jackson, Mumby, & Steneck, 2010), thereby conferring upon it low vulnerability (Mumby, Chollett, Bozec, & Wolff, 2014). In this framework, temporal trends in coral cover are the most common indicator of coral reef resilience (Mumby & Anthony, 2015), reflecting both its resistance (capacity to withstand disturbance) and recovery (the rate at which coral cover returns to its pre-disturbance level). Threats that undermine coral reef resilience can be broadly grouped into chronic stressors (such as ocean warming, pollution, sedimentation, and over-harvesting) and acute stressors or disturbances (such as coral predation by crown-of-thorns starfish (CoTS) *Acanthaster* cf. *solaris*, coral bleaching, coral disease, and tropical cyclones) that interact in complex ways (Vercelloni, Caley, & Mengersen, 2017). For example, nutrient enhancement from terrestrial runoff can increase coral susceptibility to disease and bleaching (Thurber et al., 2014), and potentially initiate outbreaks of CoTS (Fabricius, Okaji, & De'ath, 2010). Previous studies have begun to unravel the factors that make a reef more resilient, including herbivory (Hughes et al., 2007), connectivity (Hughes, Bellwood, Folke, Steneck, & Wilson, 2005), and protection from fishing (Mellin, Macneil, Cheal, Emslie, & Caley, 2016). However, the small percentage of locations where there is regular and detailed data collection represents a bottleneck for understanding resilience at scales relevant to regional conservation and management. Spatial resilience (sensu Cumming, Morrison, & Hughes, 2017), a subset of the resilience theory, focuses on processes influencing a system's ability to maintain its integrity and functions that operate across multiple locations and spatial scales, from local (e.g., environmental conditions, habitat characteristics) to regional or global (e.g., management regimes or the impact of regional disturbances exacerbated by global change). Yet there is currently no framework available for predicting which reefs are the most resilient based on spatial variation in underlying environmental, biological, and ecological processes at multiple spatiotemporal scales. Consequently, management plans are routinely designed and implemented with little capacity to quantify their effectiveness in supporting reef resilience, and to improve such plans adaptively.

Australia's Great Barrier Reef (GBR) offers a unique opportunity to disentangle the effects of acute disturbances from the impacts of fishing, which has remained low and well regulated compared to most reefs worldwide. Previous statistical assessments of historical trends for the GBR found a 50% decline in coral cover over the last three decades, mostly due to the effect of cyclones and CoTS outbreaks (De'ath, Fabricius, Sweatman, & Puotinen, 2012). However, those results were based on a subset of 214 reefs, representing 7% of the total reef area of the GBR with few inner-shelf reefs. Furthermore, this assessment did not account for coral recovery following disturbance—a critical requirement for accurately reconstructing coral trajectories and identifying key drivers of reef resilience. Recent advances have helped quantify the effect of cumulative stress on coral recovery potential (Ortiz et al., 2018); however, they were based on even fewer samples collected prior to 2010, and consequently, do not include the latest and most severe bleaching events (Hughes et al., 2017) and recent major cyclone impacts (Puotinen, Maynard, Beeden, Radford, & Williams, 2016). Only few studies thus far have attempted to identify the environmental drivers of coral growth rate (e.g., Madin, Hoogenboom, & Connolly, 2012, Pratchett et al., 2015, MacNeil et al., 2019), and none has derived high-resolution predictions of coral cover over the entire time series of available data.

Here we develop a high-resolution dynamic model of coral cover for reefs of the GBR that directly incorporates the cumulative effects of disturbances such as coral bleaching, disease, CoTS outbreaks, and tropical cyclones. By accounting for key ecological processes (coral growth and recovery potential), environmental drivers of coral cover, and observed disturbance history, we reconstruct coral cover trajectories for >1,500 reefs at a 0.01° (~1 km) resolution over the last 22 years (1996–2017). Importantly, for the first time, our model includes a spatially explicit index of water quality for the frequency of river plume-like conditions (Petus, Silva, Devlin, Wenger, & Alvarez-Romero, 2014), which can negatively affect corals (Fabricius, 2005; Wolff, Mumby, Devlin, & Anthony, 2018). We independently validate our model predictions and provide quantitative estimates of model uncertainty—a critical requirement for informing decision-making and risk analyses (Mumby et al., 2011). We use this model to map the resilience of corals to anthropogenic and natural stressors across the GBR and show that resilience was negatively related to plume conditions.

2 | METHODS

2.1 | Experimental design

Model development followed two main steps (Figure S1): (*i*) estimate the Gompertz-based model parameters from long-term surveys and predict them in every 0.01° grid cell across the Great Barrier Reef (GBR), and (*ii*) couple these spatially explicit estimates of coral cover with spatial layers of disturbance history and water quality to reconstruct coral cover trajectories between 1996 and 2017 across the GBR.

Step (*i*) involved predicting benthic communities (i.e. ecological communities composed of hard corals and other benthic organisms or abiotic substrate) based on environmental and spatial correlates

using multivariate regression trees. This was done using surveys of average benthic cover for a subset of reefs on the GBR. We then developed a Gompertz-based Bayesian hierarchical model that estimated intrinsic coral growth rate (r_s), as well as the effect of various disturbances on coral cover, for individual transects nested within survey reefs and benthic communities. From these estimates, we predicted intrinsic coral growth rate across the GBR, using boosted regression trees (BRT) based on environmental and spatial predictors. We also used our BRT model to predict the coral cover observed in 1996 (HC_{ini}) and maximum (HC_{max}) coral cover in every 0.01° grid cell based on observations at surveyed reefs.

Step (*ii*) involved predicting coral cover in each year of the time series by combining BRT predictions of HC_{ini}, HC_{max} and r_s with the impact (severity × effect size) of the various disturbance agents including coral bleaching, disease, CoTS outbreaks, tropical cyclones, and unknown disturbance. This allowed us to predict coral cover in every grid cell and in every year between 1996 and 2017. We validated model predictions using an out-of-sample, independent set of survey reefs, mapped model uncertainty and identified its main sources based on a sensitivity analysis. Last, we compared predictions of mean annual change in coral cover with an index of cumulative disturbance to quantify reef resilience, defined as the net effect of resistance and recovery following disturbance.

2.2 | Survey reefs

Australia's Great Barrier Reef (GBR) consists of more than 2,900 individual reefs extending over 2,300 km between 9 and 24°S latitude. Reef communities of the GBR have been monitored yearly between 1993 and 2005, and then biennially thereafter, by the Australian Institute of Marine Science's (AIMS) Long-Term Monitoring Program (LTMP) (Sweatman et al., 2008). As part of the LTMP, a total of 46 reefs were monitored for transect-based benthic cover between 1996 and 2017 in six latitudinal sectors (Cooktown-Lizard Island, Cairns, Townsville, Whitsunday, Swain and Capricorn-Bunker) spanning 150,000 km^2 of the GBR. In each sector (with the exception of the Swain and Capricorn-Bunker sectors) at least two reefs were sampled in each of three shelf positions (i.e., inner, mid- and outer). An additional 45 reefs were surveyed using the same methodology as part of the Representative Areas Program (RAP) (Sweatman et al., 2008), and 17 reefs as part of the Marine Monitoring Program (MMP) (Thompson et al., 2016). Finally, reef-level information on hard coral cover was collected by manta-tow for 97 reefs surveyed in 1996 and thereafter (44 of those being also surveyed for transect-based benthic cover).

We used information from the 46 LTMP reefs in every step of model development, in addition to those from other monitoring programs where possible, depending on the number of survey years and whether associated disturbance data were available (Table S2). We validated coral cover trajectories based on 10 manta-tow reefs that were not used for model calibration, and for which disturbance history as well as ≥10 years of data post-1996 were available.

2.3 | Survey methods and data collection

For LTMP and RAP, transect-based data on benthic assemblages were collected at three sites separated by >50 m within a single habitat on the reef slope (the first stretch of continuous reef on the northeast flank of the reef, excluding vertical drop-offs). Within each site, five permanently marked 50-m long transects were deployed parallel to the reef crest, each separated by 10 m along the 6–9 m depth contour. Percentage cover of benthic categories was estimated for each transect using point sampling of a randomly selected sequence of images (Jonker, Johns, & Osborne, 2008). The benthic organisms under five points arranged in a quincunx pattern in each image were identified to the finest taxonomic resolution possible (n = 200 points per transect) and the data were converted into percent cover. For MMP, the smaller size of inshore reefs dictated a reduced design that included two sites at each reef within which five 20-m long transects with n = 160 points per transect were used for estimation of percent cover. In this study, we considered the combined cover of all hard corals, hereafter referred to as hard coral cover (HC; %).

Manta-tow surveys were conducted around the perimeter of entire reefs to estimate hard coral cover and densities of CoTS (Miller & Müller, 1999). Manta-tow surveys involved a snorkeler with a "manta board" (hydrofoil) being towed slowly behind a small boat around the entire perimeter of each survey reef close to the reef crest so that the observer surveyed a 10-m-wide-swathe of the shallow reef slope (Bass & Miller, 1996). The boat stopped every 2 min to allow the observer to record the mean coral cover into one of 10 categories (Bass & Miller, 1996), giving one cover estimate per tow (~200 m of reef edge) with the number of tows per reef varying from 3 to 325 depending on reef size.

2.4 | Environmental and spatial covariates

A set of 31 environmental variables were collated across the GBR at a 0.01° resolution (12,670 grid cells, spanning a total area of 14,778 km^2) (Matthews et al., 2019). From these variables, we selected those with a reported effect on coral ecophysiology as our candidate model predictors (Table S1). These environmental variables include long-term annual averages and seasonal variation of temperature, salinity, chlorophyll a and nutrient concentrations (nitrate, phosphorus), oxygen levels and light availability, as well as sediment covers and bathymetry, which are all important predictors of coral reef and seabed biodiversity on the GBR (Mellin, Bradshaw, Meekan, & Caley, 2010; Sutcliffe, Mellin, Pitcher, Possingham, & Caley, 2014) (Table S1). In addition, spatial variables including the shortest distances to the coast and to the barrier reef were calculated for each grid cell of the GBR using great-circle distance (i.e., the shortest distance between two points on the surface of the Earth). Within this 0.01° resolution grid, reefs (polygons) were identified, using the marine bioregion classification from the Great Barrier Marine Park Authority (GBRMPA), excluding any non-reef locations (e.g., cays, islands, mangroves) and restricting coverage to depths

<30 m. The grid was truncated by removing all cells with a latitude of <12°S due to data scarcity in northernmost locations.

2.5 | Water quality

We used the average frequency of exposure to river plume-like conditions (PFc) as a proxy for exposure to dissolved nutrients and fine sediments delivered during the wet season (MacNeil et al., 2019). Based on satellite observations during the 2005–2013 wet seasons, the frequency (i.e., number of weeks per year) of exposure to primary, secondary and tertiary river plumes were estimated at a 1-km resolution (Petus et al., 2014). Primary water consists of the turbid, sediment-dominated parts of the plume, secondary water consists of the chlorophyll-dominated parts of the plume, and tertiary water consists of the furthest extent of the relatively clearer parts of the plume. Here we pooled these three water types to estimate the frequency of inundation of any plume water, expressed as a proportion of total wet season weeks.

2.6 | Disturbance data

The disturbance data included two components (*i*) point-based records of coral damage collected concurrently with the benthic surveys (e.g., Mellin et al., 2016) and (*ii*) spatial layers of disturbance history and associated severity across the GBR available in Matthews et al. (2019).

(*i*) In point-based records of coral damage, disturbances were classified into five categories (i.e. coral bleaching, CoTS outbreaks, coral disease, cyclones or unknown) following Osborne, Dolman, Burgess, and Johns (2011) based on visual assessment by experienced divers during reef-scale manta tow and intensive SCUBA surveys. A disturbance was recorded when the total coral cover decreased by more than 5% from its pre-disturbance value between two consecutive periods. Each disturbance was identified by distinctive and identifiable effects on corals, such as the presence of CoTS individuals or feeding scars, or dislodged and broken coral indicative of cyclone damage (Osborne et al., 2011). An additional category labeled "unknown" was used to classify unidentified disturbances. This dataset thus resulted in a series of five binary variables coding the presence (1) or absence (0) of each type of disturbance in each year and at each reef where transect-based surveys of benthic assemblages were conducted.

(*ii*) Spatial layers of disturbance severity during the study period were available at a 0.01° resolution for coral bleaching, CoTS outbreaks and cyclones (Matthews et al., 2019). In this dataset, per cent coral cover bleached was interpolated using inverse distance weighting (maximum distance = 1°; minimum observations = 3) from extensive aerial surveys at 641 reefs for the 1998, 2002, and 2016 mass bleaching events on the GBR (Berkelmans, De'ath, Kininmonth, & Skirving, 2004; Hughes et al., 2017). Interpolated maps of CoTS densities were also generated by inverse distance weighting (maximum distance = 1°; minimum observations = 3) from the manta tow data collected by the Australian Institute of Marine Science in every year from 1996 to 2017 (Miller & Müller, 1999). The potential for cyclone damage was estimated based on 4-km resolution reconstructed sea state as per Puotinen et al. (2016). This model predicts the incidence of seas rough enough to severely damage corals (top one-third of wave heights >4 m) caused by cyclones for every cyclone between 1996 and 2016. We then used these spatial layers to associate the binary occurrence of each disturbance resulting in coral cover loss (as per [*i*]) with its severity. Note that, at the time of writing, aerial surveys following the 2017 bleaching event as well as the impact of the 2017 tropical cyclone Debbie (based on the methodology developed by Puotinen et al., 2016) were unavailable. Due to the unavailability of spatially continuous information on the occurrence and severity of coral disease and unidentified disturbance (which both had a low influence on coral cover compared to cyclones or CoTS outbreaks), we randomly generated spatial layers for these disturbances in every year and every model simulation (N = 1,000) matching their observed frequency as per the LTMP historical records.

Disturbance impacts are typically patchy at sub-reef scales, because some sections of the reef might not be exposed to cyclone-generated waves and/or be structurally vulnerable (Puotinen et al., 2016), or because of local CoTS aggregation patterns (Pratchett, Caballes, Rivera-Posada, & Sweatman, 2014). The consequence is a discrepancy between the expected effect of disturbance from our layers and the actual coral loss recorded at each transect during LTMP surveys. To explicitly account for such sub-reef scale effects, we resampled the disturbance data in every model simulation (N = 1,000) to match the actual disturbance frequencies observed during field surveys. In other words, we "turned off" some disturbances assuming they would not result in a noticeable coral loss at the reef scale, with the frequency of these false positives (6.4% for coral bleaching; 6.9% for CoTS outbreaks and 9.6% for tropical cyclones) being determined from the LTMP disturbance history and field-based records of coral loss. We further assess model sensitivity to the adjusted disturbance data (among other sources of model uncertainty; see Model validation, uncertainty and sensitivity analysis).

2.7 | Modeling

2.7.1 | Predicting benthic communities across the GBR

We identified benthic communities using multivariate regression trees (De'ath, 2002) (MRT), which allowed us to model the relationship between spatial and environmental covariates, and the relative cover of the different benthic groups and coral taxa. MRT forms clusters of sites by repeated splitting of the data, with each split determined by habitat characteristics (De'ath, 2002) and corresponding to a distinct species assemblage. Tree fit is defined by the relative error (RE; total impurity of the final tree divided by the impurity of the original data). RE is an over-optimistic estimate of tree accuracy, which is better estimated from the cross-validated relative error (CVRE). We determined the best tree size (i.e. number of leaves or clusters formed by the tree) as that which

minimized CVRE, which varies from zero for a perfect predictor to nearly one for a poor predictor (De'ath, 2002). We then examined the splits and quantified the variance that each of them explained, based on the entire dataset and for each individual functional group. We used the resulting MRT to predict community membership for every 0.01° grid cell on the GBR based on the spatial layers available for our covariates. MRT were fit in the R package "mvpart".

We subsequently characterized each cluster by its indicator taxa based on the Dufrêne-Legendre index, which is based on the relative abundance and frequency of each benthic category within a given cluster (Dufrêne & Legendre, 1997). The index varies between 0, no occurrences of a species within a cluster, to 100, if a species occurs at all sites within the cluster and in no other cluster. The index is associated with the probability of resulting from a random pattern, based on 250 reallocations of sites among clusters (Dufrêne & Legendre, 1997).

2.7.2 | Gompertz model of coral growth

We reconstructed coral cover trajectories over the last 22 years (1996–2017) for every 0.01° grid cell based on the parameters estimated from a Gompertz-based Bayesian hierarchical model of coral growth previously fitted to the LTMP reefs (MacNeil et al., 2019). This growth model is an adaptation of the Gompertz-based model of benthic cover developed by Fukaya et al. (Fukaya, Okuda, Nakaoka, Hori, & Noda, 2010) that quantifies the intrinsic growth rate (r_s) and strength of density dependence (α) for sessile species, expressed as coverage of a defined sampling area. In our case, this was the percentage of visual points that contained hard coral within the LTMP data per transect (HC_t). Using a Binomial (BIN) observation model, we assumed a hierarchy where transect level observations (i) at time (t), were nested within reef (r), nested within each benthic community (c):

$$HC_{crt,i} \sim BIN(100, p_{c,r,t,i})$$

with mean model:

$$\begin{aligned}\log(p_{c,r,t,i}\times 100) = {} & r_{s,cr} + (1-\alpha_{c,r})\log(HC_{c,r,t-1,i}) + \sum_i \beta_i\, Disturb_{i,t} \\ & + \sum_i \beta_{i.CA}\, Disturb_{i,t}\times CA_r + \sum_i \beta_{i.PFc}\, Disturb_{i,t}\times PF_{c,r}\end{aligned} \quad (1)$$

and where

$$\alpha_{c,r} \sim N(\alpha_c, \sigma_{\alpha c})$$

$$r_{s,c,r} \sim N(r_{s,c} + k_0 CA_r + k_1 PF_{C,r}, \sigma_{rc})$$

$$\alpha_c, r_{s,c}, k_0, k_1, \beta_i \sim N(0,100)$$

$$\sigma_{\alpha c}, \sigma_{rc} \sim U(0,100)$$

where r_s is the intrinsic growth rate, α is the strength of density dependence, β_i is the effect size of the ith disturbance occurring in year t ($Disturb_{i,t}$; i.e. bleaching, CoTS outbreak, disease, cyclone or unknown), CA is a binary indicating which reefs are located in a closed (i.e. no-take) area, PF_c is the water quality proxy for river plume-like conditions (Petus et al., 2014) and β_{PFc} its effect size, and $\beta_{i.CA}$ and $\beta_{i.PFc}$ are the effect size relating to interactions between disturbances and CA and PF_c respectively. Our model was thus built at a yearly resolution, assuming that any reduction in coral cover measured during a survey (i.e. above the 5% threshold) reflected the impact of a disturbance occurring between that survey and the previous one. We did not include interactions among disturbances because only <1% of all grid cells were affected by two disturbances within the same year, with insufficient instances of LTMP reefs being exposed to co-occurring disturbances during the study period. Note that in this formulation, each benthic community had their own global mean at the top of the hierarchy.

In the absence of disturbance, coral cover increases from its initial value (HC_{ini}, in 1996 in our case) to its asymptote (HC_{max}, determined by the reef carrying capacity or amount of available substrate in grid cell i) where

$$\lim_{t\to\infty} HC_t = \lim_{t\to\infty} HC_{t-1} = HC_{max} \quad (2)$$

which, once combined with Equation , gives

$$\alpha = \frac{r_s}{HC_{max}} \quad (3)$$

Because the strength of density dependence (α) depends on the intrinsic growth rate (r_s) (Fukaya et al., 2010), for which we needed separate predictions in each grid cell, we elected to predict HC_{max} (rather than α) in each grid cell using the same modeling technique to avoid circularity, and calculated α based on Equation 3.

Those models were run in a Bayesian framework, using the PyMC3 package in Python (Salvatier, Wiecki, & Fonnesbeck, 2016), with inferences made from 5,000 samples of the default No U-Turn Sampler (NUTS) algorithm. Parallel chains were run, from starting values initialized automatically by an Automatic Differentiation Variational Inference (ADVI) algorithm, to look for convergence of posterior parameter estimates using the Gelman–Rubin convergence statistic (R-hat); posterior traces and predictive intervals were also examined for evidence of convergence and model fit.

2.7.3 | Predicting coral growth rate (r_s), initial (HC_{ini}) and maximal (HC_{max}) cover across the GBR

We predicted r_s, HC_{ini} and HC_{max} in each 0.01° grid cell from observed values at the survey reefs and as a function of spatial, environmental and disturbance-based correlates using boosted regression trees (BRT). BRT is a machine learning algorithm that uses many simple decision trees to iteratively boost the predictive performance of the final models (Elith, Leathwick, & Hastie, 2008). Model settings include the learning rate (l_r) that controls the contribution of each tree to the final model and tree complexity (t_c) that determines the extent to which interactions were fitted. The number of trees (n_t)

that achieved minimal predictive deviance (i.e., the loss in predictive performance due to a suboptimal model) was determined using cross-validation (Elith et al., 2008) (function gbm.step with t_c = 2, l_r = 0.001, bag fraction = 0.5).

We assumed a Gaussian error distribution in all three BRT, after a logit-transformation of HC_{ini} and HC_{max} to achieve normality (no transformation was required for r_s). In addition to spatial and environmental predictors, we used past disturbance history over a 10-year period based on evidence that some disturbance impacts can have temporally lagged and lasting effects on coral communities over this timeframe (Mellin et al., 2016). We thus included the mean cyclone severity and the mean CoTS density between 1985 and 1995 to predict the coral cover observed in 1996 (HC_{ini}); and the mean cyclone severity, CoTS density during 1996–2016 in addition to the per cent coral bleached in 1998, 2002, and 2016 to predict the maximum coral cover observed between 1996 and 2017 (HC_{max}). Because r_s estimates already accounted for the influence of past disturbance (filtered out by disturbance parameters in the Bayesian hierarchical model), we only accounted for spatial and environmental variables in this BRT to avoid circularity.

The relative contribution of the predictors to the final models of HC_{ini}, HC_{max} and r_s was determined based on the variable importance score (%). For each response variable, the mean prediction error was assessed using a 10-fold cross-validation (Davison & Hinkley, 1997). This bootstrap resampling procedure estimates a mean prediction error for 10% of observations that were randomly omitted from the calibration dataset; this procedure was iterated 1,000 times. We also verified that model residuals were not spatially autocorrelated using Moran's *I* and a Bonferroni correction ($p > 0.05$) (Diggle & Ribeiro, 2007). Finally, we generated a set of 100 model predictions across the GBR and calculated mean estimates of HC_{ini}, HC_{max} and r_s and their standard deviation in each cell. BRT were fit in R 3.2.2 (R Development Core Team, 2017) using the "gbm" package, along with the tutorial and functions provided in Elith et al. (2008).

2.7.4 | Correction of systematic bias in manta-tow estimates

To improve model predictive power and spatial representation, we used data from the manta tow surveys (in addition to the transect-based LTMP data) for calibrating BRT of HC_{ini} and HC_{max} (Table S2). However, due to a moderate yet systematic bias of manta-tow coral cover estimates being lower than transect-based ones (resulting from non-coral habitats such as sandy back-reef lagoons being included in the manta tow; Osborne et al., 2011), we first had to derive a corrected manta-tow estimate of coral cover accounting for this bias. We thus fitted a linear regression predicting transect-based coral cover (averaged to the reef level) as a function of manta tow-based coral cover, using data from the 44 reefs that were sampled both by manta-tow and along transects. We then used this regression to predict a corrected estimate of observed coral cover for all reefs surveyed by manta-tow, which we could then compare to transect-based coral cover estimates. For both datasets, we defined initial coral cover at each reef (HC_{ini}) as the mean coral cover observed in 1996 across all transects, and the maximum coral cover (HC_{max}) as the highest mean coral cover observed at that reef between 1996 and 2017.

2.7.5 | Model validation, uncertainty and sensitivity analysis

We validated predicted coral cover trajectories by comparing them with corrected manta-tow estimates of coral cover for reefs that were not used for model calibration, and for which at least 10 yearly samples were available from 1995 along with the associated disturbance history (N = 10). Based on these 10 time series, we calculated the mean prediction error (*PredErr*, %) and the coefficient of determination based on the regression of predictions against observations (R^2, %).

We identified areas where model predictions were interpolated (thus resulting in high confidence in model predictions (Elith & Leathwick, 2009, Yates et al., 2018) and those where predictions were extrapolated (lower confidence). We used a common procedure to identify the environmental envelope used for model calibration based on a principal component analysis (PCA) (e.g., Broennimann et al., 2007, Medley, 2010) with environmental and spatial predictors at the survey reefs as input variables, and the 12,670 grid cells as individuals. Based on the PCA individual factorial plan, we outlined the modeled environmental envelope as the convex hull containing all survey reefs. Grid cells falling within this environmental envelope were defined as interpolated locations; conversely, those outside this envelope were considered part of the extrapolation areas.

To account for model uncertainty, we ran a total of 1,000 model simulations in which we resampled every parameter from their predicted distribution. We used Latin hypercube sampling (Norton, 2015) (R package "lhs") to determine a total of 1,000 combinations of percentiles, evenly spread out in the new parameter space, which we used to draw a single value for r_s, HC_{ini}, HC_{max} and the disturbance effect sizes (from their posterior distributions) in each simulation. The resulting predictions of coral cover in every grid cell (rows), year (columns) and model simulation were stored as 3D arrays and further aggregated across the third dimension to derive coral cover statistics across model simulations (mean, median, interquartile range and 95% confidence interval). We mapped model uncertainty as the coefficient of variation (%) in predicted mean annual change in coral cover across all simulations.

Finally, we ran a sensitivity analysis to identify, among all model parameters, the main sources of model uncertainty and any possible interactions among them (Pearson et al., 2014). In this analysis, we used the mean annual change in coral cover predicted in each simulation as the response variable, and the (resampled) parameter estimates used in each simulation as the predictors of a boosted regression tree. This analysis allowed us to quantify the proportion of model uncertainty that is attributable to variation in parameter estimates (i.e., percent deviance explained by the BRT), the respective contribution of each model parameter (i.e., relative importance of each predictor, %) and possible interactions among them (Norton, 2015).

2.7.6 | Mapping coral resilience

We mapped coral resilience (i.e., the net effect of resistance and recovery following disturbance) based on the relationship between predicted mean annual decline in coral cover and cumulative impacts of mean annual disturbance at each reef. To do this, we calculated the cumulative disturbance index in each grid cell as the sum of all cyclones, bleaching and CoTS outbreak severities weighted by their respective effect sizes from the Bayesian HLM. We defined categories of low/high decline, and low/high disturbance, based on the median of each index.

We defined resilience as the second axis of a PCA based on predicted decline in coral cover and cumulative disturbance for all reefs (PC2; 21% variation explained). Reefs with relatively low decline following high disturbance (i.e., high resilience reefs) scored positively on PC2, while reefs with high decline following low disturbance (i.e., low resilience reefs) scored negatively. For this analysis, we excluded reefs located in extrapolated areas, for which we had lower confidence in model predictions.

We investigated the relationship between coral resilience and potential anthropogenic covariates that included our water quality index (PF_c), an index of reef accessibility based on potential travel time from nearest human settlements (Maire et al., 2016), and whether a reef was designated as a no-take marine protected area based on the 2004 zoning plan by the Great Barrier Reef Marine Park Authority. We fitted a generalized additive model (Hastie & Tibshirani, 1990) to model the relationship between coral resilience and PF_c, and that between resilience and reef accessibility, using a Gaussian error distribution and a cubic spline smoothing function ($k = 3$). We tested whether coral resilience differed among no-take reefs and those open to fishing using a non-parametric Kruskal–Wallis test. All code was written in R (R Development Core Team, 2017) (except for the Gompertz model in Python; see corresponding section) and is provided in Supplementary Information.

3 | RESULTS

3.1 | Regional impacts of disturbance on the GBR

The impact of tropical cyclones, CoTS outbreaks, and coral bleaching on coral cover varied greatly in space and time across the GBR (Figure 1). Based on the 46 reefs regularly surveyed by the AIMS Long-Term Monitoring Program (LTMP), our Bayesian hierarchical model showed that tropical cyclones had the strongest, most consistent negative effect on coral cover, followed by CoTS outbreaks and coral bleaching (Figure S2). By combining these effect sizes with high-resolution maps of annual disturbance severity, we were able to predict the impacts of each disturbance on coral cover across the GBR from 1996 to 2017 (Figure 1a–c) and show regional differences in how these disturbances likely impacted individual reefs.

Cyclone impact was greatest between Townsville and Mackay (Figure 1a), where tropical cyclones Hamish (2009) and Dylan (2014) generated some of the longest-lasting destructive waves (Figure S3). CoTS outbreaks propagated in a southerly direction from reefs north of Cairns (Figure S3), and formed a second localized concentration further south. The highest CoTS densities on average (and thus the largest CoTS impact on coral cover) were recorded off Townsville and on offshore reefs between Mackay and Rockhampton (Figure 1b). The impact of coral bleaching, based on aerial surveys following the three mass coral bleaching events (1998, 2002, and 2016), was greatest on the northern half of the GBR (Figure 1c), a pattern that was mostly driven by the latest and most severe bleaching event (Figure S2).

Our coral cover predictions closely followed spatiotemporal trends in disturbance impacts, with the greatest decline in coral cover predicted for central reefs mostly impacted by cyclones and, to a lesser extent, northern reefs impacted by both cyclones and bleaching (Figure 1d). Between 1996 and 2017, we predicted an increase in coral cover for approximately 10.2% of the total reef area, mostly for southernmost reefs that were less impacted by cyclones and bleaching (note this calculation excludes reefs for which predictions were extrapolated as this results in low confidence—these areas are enclosed within grey outlines on Figure 1d).

Between 1996 and 2017 and across the breadth of the GBR, coral cover declined at a mean annual rate of −0.67%/year (Figure 1f). This decline was steepest towards the end of the time period (2009–2016; −1.92%/year), reflecting a response of hard corals to multiple severe and widespread cyclones (including Hamish in 2009, Yasi in 2011, and Dylan in 2014) and to the 2016 mass coral bleaching event (Figure 1e). Coral cover also markedly declined between 1996 and 2002 (−0.75%/year), which encompassed mass bleaching events in 1988 and 2002 and a major CoTS outbreak (Figure S2). In between those time periods, mean coral cover increased by +0.73%/year on average (2003–2009).

3.2 | GBR-wide recovery

Coral recovery potential varied among the different coral communities, which we identified from the survey data and predicted across the GBR using MRT. Among candidate MRT predictors, the distance to the outer barrier reef edge, as well as seasonal variation in sea surface temperature and seabed oxygen concentration (strongly correlated to the latter: Spearman's $\rho = 0.61$, $p < 0.001$) were the main predictors of benthic community composition (Figure S4). Using this model, we were able to define 6 benthic community types across the GBR, which consisted of major functional groups of corals as well as other benthic organisms or abiotic substrate. Outer-shelf communities were characterized by the fast-growing tabular or digitate *Acropora spp.*, as opposed to inner-shelf communities that were characterized by *Porites* or macroalgae (Figure 2).

Our Gompertz-based Bayesian hierarchical model revealed that the frequency of river plume conditions (PF_c) had a strong negative effect on coral intrinsic growth rate (r_s), which was higher for outer-shelf communities characterized by tabular or digitate *Acropora* spp. (Figure S2). Accordingly, high-resolution predictions of r_s derived from the BRT across the GBR increased from inner- to outer-shelf

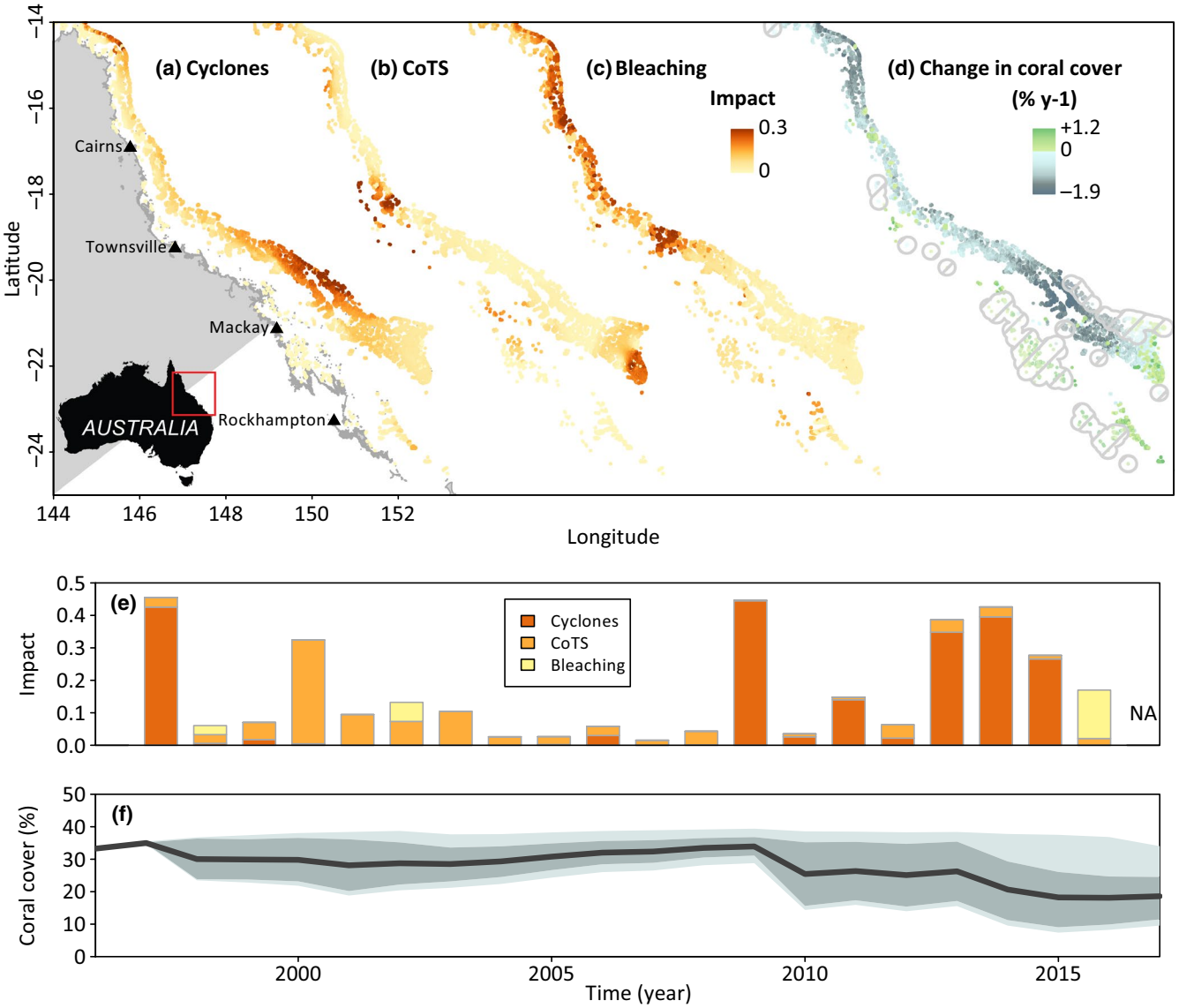

FIGURE 1 Regional impact of major disturbances on the Great Barrier Reef and resulting trends in coral cover. Average 1996–2017 impact of (a) tropical cyclones, (b) outbreaks of the crown-of-thorns starfish (CoTS), and (c) coral bleaching (note that only the three mass bleaching events were considered). (d) Mean predicted annual rate of change in coral cover (%/year) during the same period, with greyed out areas indicating lower confidence in model predictions due to extrapolation. (e) Relative impact of each disturbance in each year. (f) Mean predictions of coral cover averaged across the entire Great Barrier Reef; envelopes indicate the 95% confidence interval across a total of 1,000 simulations (light hue), the interquartile range (medium hue) and the mean trajectory (dark continuous line) [Colour figure can be viewed at wileyonlinelibrary.com]

reefs, with 76% of deviance in r_s posterior estimates explained by the BRT (Figure 2a) and a mean cross-validated prediction error of 21%.

The distance to the reef edge (strongly correlated to PF_c; Spearman's $\rho = 0.63$, $p < 0.001$) was the main predictor of coral growth rate (20% relative importance), followed by the benthic community (10%), and seasonal variation in salinity and sea surface temperature (9% each) (Figure 2b). Predicted coral growth rate was the highest for outer-shelf communities characterized by tabulate and digitate *Acropora* spp., and the lowest for inner-shelf communities with relatively high macroalgal cover (Figure 2c). The fastest-growing communities characterized by tabulate and digitate *Acropora* spp. were concentrated in 2.1% of the study area overlapping the outer edge of the GBR (Figure 2a).

Our spatially-explicit predictions of other Gompertz parameters, namely initial (i.e., HC_{ini}, in 1996) and maximum (HC_{max}) coral cover at each reef, showed that BRT explained 78% and 80% of the deviance in HC_{ini} and HC_{max} at survey reefs, respectively (Figure S5). The mean cyclone severity between 1985 and 1995 had the strongest negative effect on HC_{ini}, followed by mean seabed temperature. Seasonal variation in salinity was a major driver of HC_{max} at a regional scale, followed by longitude (reflecting cross-shelf environmental gradients in multiple environmental variables that increased or decreased with longitude). Mean cross-validated prediction error was 5% and 11% for initial and maximum cover respectively, with high confidence in predictions within interpolated locations (64% of the study area) (Figure S5).

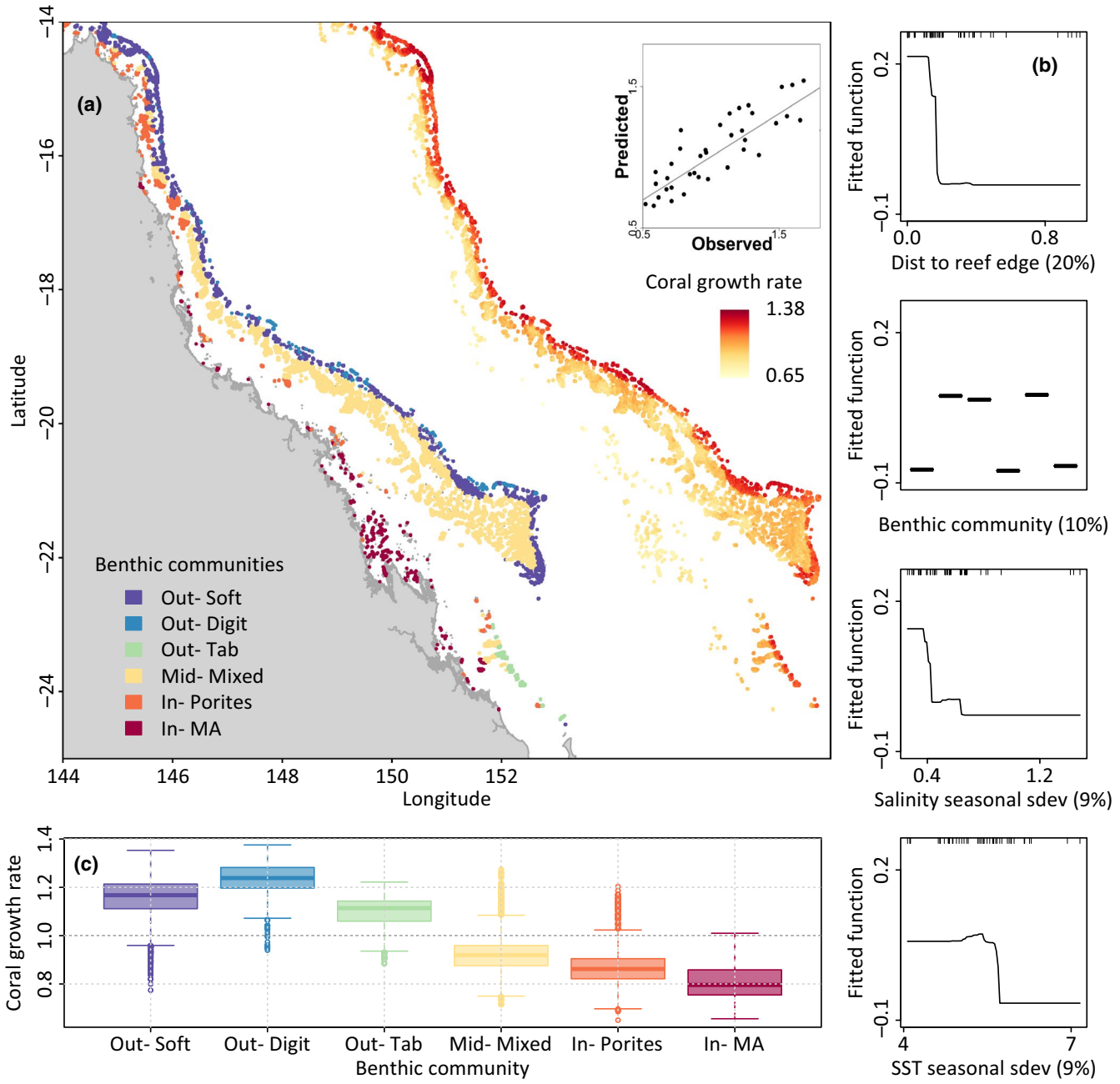

FIGURE 2 Great Barrier Reef (GBR)-wide predictions of benthic communities and coral intrinsic growth rate. (a) Benthic communities (left) and coral growth rate (right) were predicted based on major environmental covariates using multivariate (MRT) and boosted (BRT) regression trees, respectively. The insert shows the relationship between posterior estimates of coral growth rate from the Gompertz model for the LTMP reefs, used as observations in the BRT, and BRT predictions. (b) Marginal plots showing the partial effect of major environmental drivers on coral growth rate (with SST = sea surface temperature, sdev = standard deviation). The relative importance of each BRT predictor (%) is indicated in brackets. (c) Distribution of coral growth rate predicted by BRT among benthic communities. The thick line indicates the median, hinges the interquartile range, whiskers the 90% confidence interval and dots the outliers [Colour figure can be viewed at wileyonlinelibrary.com]

3.3 | Mapping coral resilience across the GBR

Based on our cumulative disturbance index that represented the combined impacts of tropical cyclones, CoTS outbreaks, and bleaching, most reefs experiencing low disturbance were predicted to show low decline in coral cover, and vice versa (Figure 3a). However, 15% of all reefs experienced strong decline following low disturbance, indicating they were low-resilience reefs. Conversely, 17% of all reefs exhibited low decline following high disturbance, thus representing high-resilience reefs. The latter were mostly located in the southernmost (and northernmost to a lesser extent) sections of the GBR, with a few clusters in the central GBR (dark green on Figure 3a).

Reef resilience was strongly and negatively related to the frequency of river plume-like conditions (general additive model; 14.7% deviance explained; Figure 3b), and to reef accessibility to a lesser extent (3% deviance explained; Figure 3c). When all reefs were

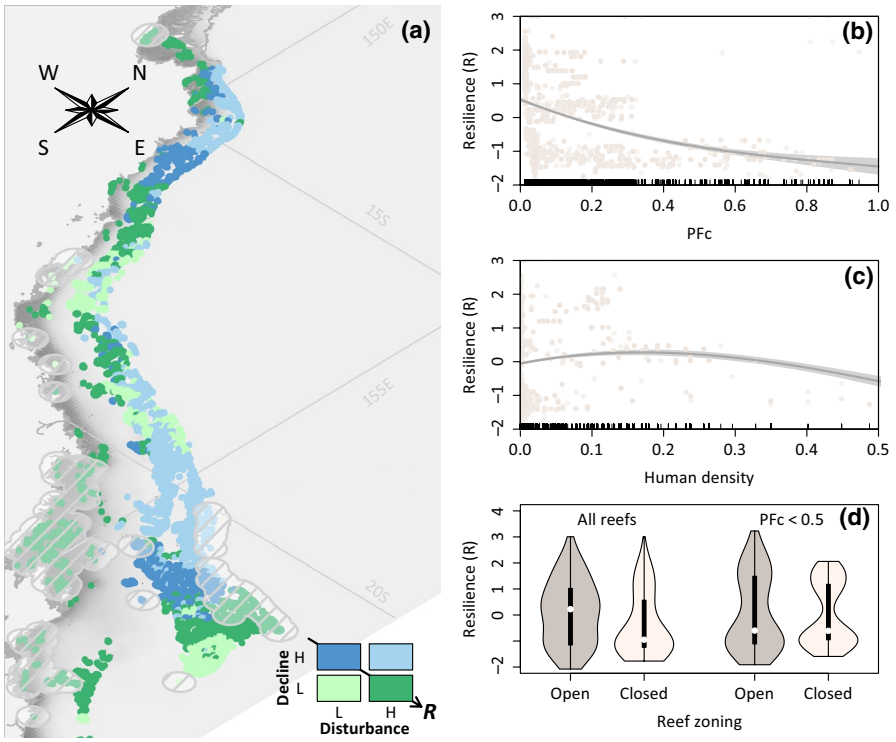

FIGURE 3 Map and correlates of coral resilience on the Great Barrier Reef. (a) Mean annual decline in coral cover versus mean annual disturbance impact (i.e. the combined severity of all coral bleaching events, CoTS outbreaks, and cyclones recorded over the study period, and weighted by their effect size). Low and high categories corresponded to values below and above the median, respectively. High-resilience reefs are characterized by low decline in coral cover following high disturbance, as shown by the resilience gradient (*R* arrow) used to assign a resilience value to each reef (see Methods). The intensity of the grey shading is proportional to the frequency of river plume-like conditions (PF_c). (b) Relationship between coral resilience and PF_c. The regression line was fitted using a general additive model (GAM), with the envelope showing the 95% confidence interval. (c) Relationship between coral resilience and reef accessibility (measured as potential travel time from major coastal cities) and GAM fit. (d) Distribution of coral resilience between open and closed (i.e. no-take) reefs, either considering all reefs (left) or only those with less frequent exposure to plume-like conditions (right; $PF_c < 0.5$). The white dot indicates the median, the vertical black bar the interquartile range, and plot width represents the proportion of all reefs [Colour figure can be viewed at wileyonlinelibrary.com]

considered, reef resilience was substantially lower on closed reefs (i.e. within no-take marine protected areas) compared to open reefs (Kruskal–Wallis test; $p < 0.001$) (Figure 3d). Most closed reefs were associated with less frequent plume-like conditions (lower median PF_c) than open reefs; however the distribution of PF_c was skewed and resulted in greater mean PF_c within closed reefs (Figure S6). When reefs with greater exposure to plume-like conditions were removed from the analysis, resilience did not differ between closed and open reefs (Figure 3d; $PF_c < 0.5$; $p = 0.412$) although r_s remained substantially higher within closed reefs (Figure S6; $PF_c < 0.5$; $p < 0.001$).

3.4 | Model validation, uncertainty and sensitivity analysis

Projected coral trajectories closely matched historical records for 10 reefs surveyed using manta-tow that were not used for model calibration (Figure 4). For this independent dataset, our model accurately captured the impact of multiple disturbances and subsequent coral recovery (mean prediction error = 6.7%; $R^2 = 0.57$). When considering all reefs with at least 10 years of coral cover data available ($N = 54$), the mean prediction error was 5.8% and the goodness-of-fit (R^2) was 0.64. Uncertainty in model predictions tended to be higher in the case of rare yet severe disturbances (e.g., Ben Reef; Figure 4) compared to multiple, less severe ones (e.g., Credlin or Feather Reefs; Figure 4). We mapped the coefficient of variation in predicted annual change in coral cover across all simulations and found that average model uncertainty was 33.6% (ranging 0.7%–84.4%). The lowest uncertainty occurred at survey reefs and the highest in central sections of the GBR distant from them (Figure S7).

Our sensitivity analysis revealed that predicted coral decline was the most sensitive to variation in r_s (BRT relative importance = 75%) followed by HC_{ini} (8.9%) and tropical cyclone impact (4.9%) (Figure S8). We found a weak interactive effect of r_s and HC_{ini} on overall patterns of predicted coral decline, with this effect being greatest at low r_s combined with high HC_{ini} (Figure S8).

4 | DISCUSSION

By reconstructing coral cover trajectories at a fine spatial resolution across Australia's Great Barrier Reef (GBR) over the last 22 years, we provide the most comprehensive, spatially explicit estimate of

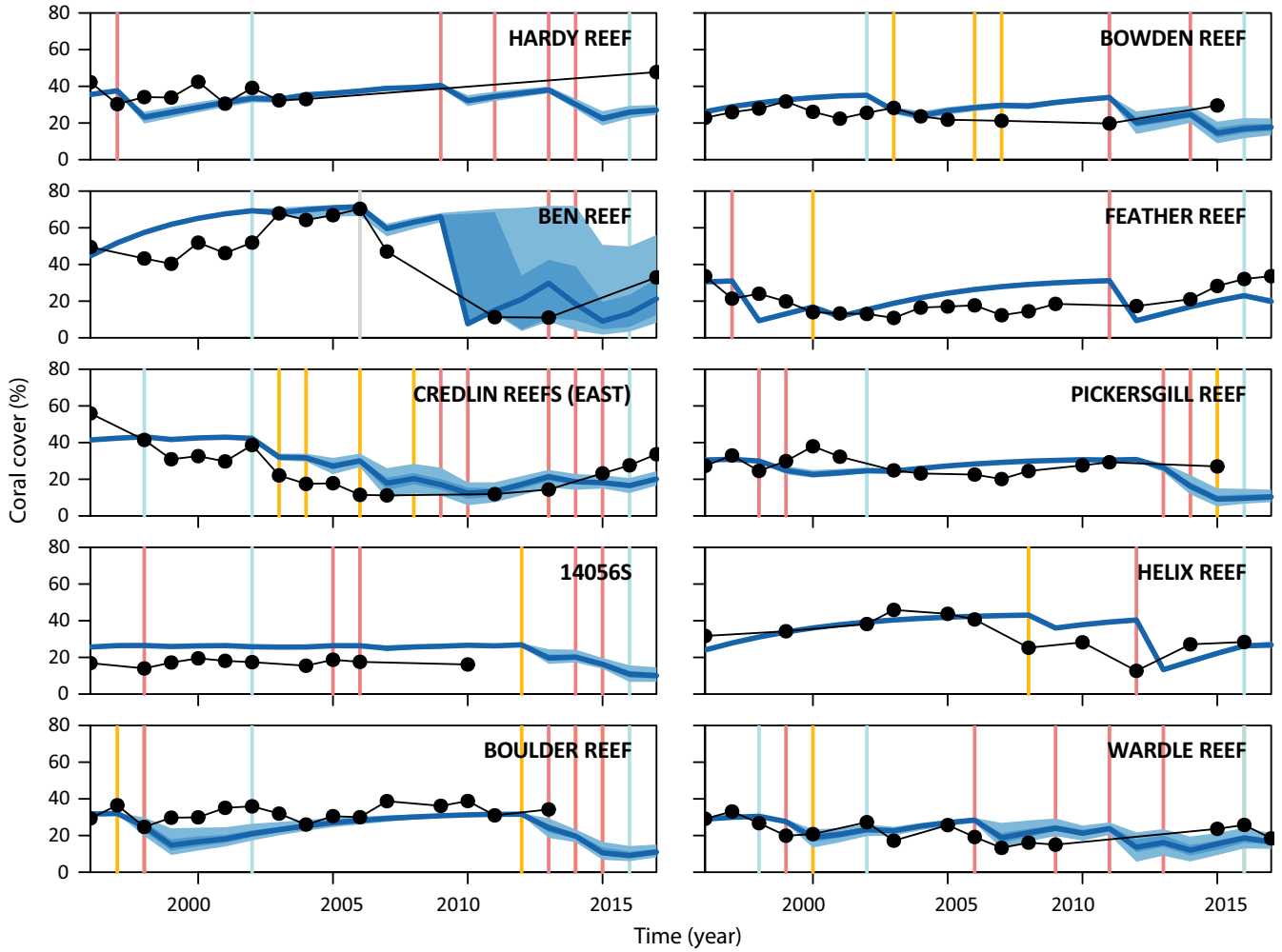

FIGURE 4 Model validation. Predicted trajectories of coral cover (blue envelopes) compared with independent observations (black dots) for manta-tow reefs. Light blue envelopes indicate the 95% confidence interval across 1,000 simulations; medium blue envelopes show the interquartile range (25th and 75th percentiles), and the dark blue line shows the median. Vertical lines indicate disturbances with blue = coral bleaching, orange = crown-of-thorns starfish outbreak, red = tropical cyclone, grey = coral disease [Colour figure can be viewed at wileyonlinelibrary.com]

long-term coral cover trajectories for any marine system, and disentangle the relative impact of multiple agents of disturbance on coral growth at local-to-regional scales. We show that coral cover is likely to have declined on 90% of all reefs. Historically, this decline has primarily been attributed to tropical cyclones and CoTS outbreaks (De'ath et al., 2012), and in more recent years to coral bleaching (Hughes et al., 2017). High water quality correlates strongly with coral resilience, with low reef accessibility (remoteness) also having a positive, albeit weaker, association. Surprisingly, reef resilience was substantially lower within no-take marine protected areas; however, this difference was driven by the effect of water quality and was not evident among reefs with less frequent exposure to plume-like conditions. We have high confidence in these results because model predictions closely matched independent observation records. By incorporating the main environmental drivers of coral cover and its growth rate into a disturbance-based model of coral decline and recovery, we offer a new and robust framework for similar applications to other reef regions around the world—a critical requirement for sustainable reef management over the coming decades (Hughes et al., 2017).

Tropical cyclones were the strongest driver of coral cover on the GBR over the last 22 years, which stems from a combination of greater effect size and frequency compared to CoTS outbreaks or bleaching. Only a broad-scale and high-resolution approach such as ours that explicitly maps spatial variation across individual reefs could reveal these spatiotemporal patterns, because most of the cyclone impacts occurred within unmonitored reef sections (e.g., Figure S2) that were not considered in previous studies (De'ath et al., 2012; Osborne et al., 2017). The stronger effect size of cyclones likely reflects that cyclones typically alter habitat structural complexity immediately, unlike other disturbances that can leave coral skeletons intact (Osborne et al., 2017). This loss of habitat complexity affects a range of coral-associated organisms such as herbivorous fishes and invertebrates that otherwise facilitate coral recruitment and recovery through grazing (Cheal, Macneil, Emslie, & Sweatman, 2017; Osborne et al., 2017). In contrast, coral cover generally recovers faster following CoTS outbreaks because the coral skeletons that remain in place provide suitable habitat for coral recruits and can sometimes shelter remnants of healthy living coral (Osborne et al., 2017).

In our study, the relatively smaller effect of bleaching is partly due to the most severe bleaching event (2016) being only recent (compared to 14 years of cyclone impacts out of a total of 22 years considered), as well as the possibility that some corals might have regained their symbionts and recovered by the time LTMP surveys were conducted. Furthermore, sampling bias might have reduced our estimates of bleaching impacts as we excluded the northernmost reefs (where bleaching impacts were the most severe) due to data paucity, and calibrated our model using observations from the 6-9m depth zone. Corals at these depths might have escaped the most damaging effects of bleaching, which were typically observed on shallow reef flats and crests where low water mixing allowed little cooling from deeper waters (Hughes et al., 2017). However, such spatial patterns of coral bleaching on shallow reefs are typically patchy (up to a 10-100m scale; S. Heron, unpublished data) and are currently difficult to resolve at the scale of the GBR. Given that coral bleaching is predicted to increase both in frequency and severity over the next decades (van Hooidonk et al., 2016; Wolff et al., 2018), its impact on coral cover will also likely increase and potentially surpass that of tropical cyclones in the future.

Lower coral resilience coincided with a greater exposure to river plume-like conditions, suggesting that water quality could play an important role in exacerbating the effect of cumulative disturbances and synergies among them. Indeed, chronic stress related to land run-off and poor water quality can affect the functional diversity of benthic communities and result in a loss of resilience (Wolff et al., 2018), potentially aggravating the impact of subsequent acute disturbances (Ortiz et al., 2018; Osborne et al., 2017). Although many indicators of water quality exist, our results indicate that nutrient and suspended sediment concentrations (as predicted by plume-like water body characterization; Petus et al., 2014) are likely to have a strong negative effect on coral cover and, therefore represent a key management priority (Brodie & Pearson, 2016). Conversely, high coral resilience characterized reefs that were previously identified as small and isolated (Mellin, Huchery, Caley, Meekan, & Bradshaw, 2010), and thus less prone to deleterious, collateral effects from disturbances at neighbouring reefs. For example, isolated reefs are typically exposed to reduced levels of colonization by CoTS larvae (Hock, Wolff, Condie, Anthony, & Mumby, 2014), representing important spatial refugia from outbreaks that tend to propagate along prevailing currents (Pratchett et al., 2014). Identifying the exact drivers of coral resilience warrants further investigation, yet the clear spatial pattern in their distribution suggests that the relative importance of terrestrial influence, cross-shelf location, and spatial connectivity could play a key role in determining coral resilience to multiple disturbances.

Assessing spatial resilience is an important step toward prioritizing areas for future reef management and conservation, whether the objective is to rescue the weakest or protect the healthiest reefs first (Game, Mcdonald-Madden, Puotinen, & Possingham, 2008). Yet the effect of no-take marine protected areas on reef resilience was strongly determined by water quality, with lower resilience within no-take areas when all reefs were considered. In contrast, when reefs frequently exposed to plume-like conditions were excluded from the analysis, resilience did not differ between no-take or open areas and r_s, our proxy for recovery potential in the absence of disturbance, was higher within no-take areas. This corroborates earlier results suggesting that marine protected areas have the potential to promote reef resistance and recovery following disturbance (Mellin et al., 2016). The survey design of this earlier study was essentially paired within and outside no-take marine protected areas, with inshore reefs being underrepresented. Another study of inshore reefs found that coral cover was lower within no-take areas than on reefs open to fishing, especially after major flooding events, indicating that repeated exposure to reduced water quality impairs reef recovery following disturbance, regardless of their protection status (Wenger et al., 2016). Together, these results indicate that while no-take marine protected areas have the potential to promote reef resilience due to increased intrinsic growth rate of corals, this potential might not suffice to counteract the deleterious effect of frequent plume-like conditions on reef resilience, suggesting that the location and environmental context of marine protected areas strongly determine their net benefit in terms of resilience.

Assessing the spatial resilience of the GBR has so far remained elusive and understandably ignored in the design of protective zoning. The southern region of the GBR, where we identified most high-resilience reefs, was previously predicted to act as a spatial refuge that will experience warming later than other coral reefs of the GBR and beyond (van Hooidonk, Maynard, & Planes, 2013). Such delayed warming in the southern GBR could contribute both to reduced bleaching-induced mortality, and reduced sub-lethal effects of thermal stress that can lead to lower coral growth rates (Osborne et al., 2017), fecundity, and resistance to disease over many years. Furthermore, more gradual warming may allow a shift to more resistant algal symbionts (Day, Nagel, Oppen, & Caley, 2008), thus facilitating the selective emergence of more heat tolerant communities (Hughes et al., 2017). Our finding of greater resilience in some areas of the southern GBR corroborates the potential for opportunities to intervene and enhance coral resilience through the integration of assisted evolution into coral reef restoration elsewhere on the GBR (van Oppen et al., 2017). However, future forecasts predict that even this "protective" thermal tolerance induced by sub-lethal bleaching events might soon be lost under current climate change (Ainsworth et al., 2016) if the increased frequency of temperature anomalies outpaces the capacity of reefs to acclimatize and adapt to novel climatic conditions. This means that, ultimately, reducing carbon emissions and mitigating global warming represent the only ways to secure reef persistence in the long term (Hughes et al., 2017).

Environmental gradients accounted for 76% of variation in coral growth rate (the most influential parameter in our coral cover model), indicating that regional scale assessments based on comprehensive environmental data are key to capturing both the drivers and spatial patterns of coral cover decline and recovery. Low seasonal variation in salinity, temperature and oxygen levels were associated with the fastest growing coral communities, characterized by tabulate and digitate *Acropora* corals among others. This result seems intuitive, given that these taxa are characterized by a "competitive" life history that can dominate communities in suitable environments, but are also very sensitive to environmental changes such as temperature anomalies

(Darling, Alvarez-Filip, Oliver, Mcclanahan, & Cote, 2012). Temperature gradients are among the main natural drivers of species distributions, affecting somatic growth and body size (Lurgi, Lopez, & Montoya, 2012), and directly reflecting the physiological influence that temperature exerts on individual species (Mellin, 2015). Furthermore, the importance of seasonal variation in oxygen levels as a determinant of benthic communities indicates that different taxa respond differently to oxygen depletion (Pitcher et al., 2012), which can reduce coral calcification rates (Colombo-Pallotta, Rodriguez-Roman, & Iglesias-Prieto, 2010) and appeared strongly temperature dependent in our data. However, modeling coral growth rate across the breadth of the GBR was also greatly improved by including spatial variables (such as the distance to the reef edge) that can provide a proxy for environmental gradients either not considered or poorly estimated (Mellin, 2015).

Based on 20 years of data, our model provides a platform for projecting coral cover trajectories under past and future scenarios of climate change, which has and will continue to affect the frequency and severity of coral bleaching (van Hooidonk et al., 2016), tropical cyclones (Walsh et al., 2016) and CoTS outbreaks (Uthicke et al., 2015). The critical question remains whether and when the capacity of reefs to absorb and recover from disturbances might be outpaced by future changes in these disturbance patterns. Our modeling approach is broadly applicable across reef ecosystems, especially given that relevant environmental and spatial layers are now increasingly available through the routine use of remotely sensed products (Mellin, Andrefouet, Kulbicki, Dalleau, & Vigliola, 2009). Our framework thus provides the advance needed to forecast which reefs will remain as important refugia for sustaining coral reef ecosystems under increasing pressures from global change.

DATA AND MATERIAL AVAILABILITY

The data and code used in this study are available at https://www.dropbox.com/s/2b6s5epx6mpokc5/Coral%20cover%20model.zip?dl=0

ACKNOWLEDGEMENTS

We thank members of the Australian Institute of Marine Science Long-Term Monitoring Program that have contributed to collection of the data used in these analyses; and B Shaffelke, K Fabricius, S Connolly, S Heron and J Brodie for providing helpful comments. This publication was supported through funding from the Australian Government's National Environmental Science Programme. CM was funded by an ARC grant (DE140100701).

ORCID

Camille Mellin https://orcid.org/0000-0002-7369-2349
Kate Osborne https://orcid.org/0000-0002-9804-6335
Nicholas H. Wolff https://orcid.org/0000-0003-1162-3556
Damien A. Fordham https://orcid.org/0000-0003-2137-5592

REFERENCES

Ainsworth, T. D., Heron, S. F., Ortiz, J. C., Mumby, P. J., Grech, A., Ogawa, D., … Leggat, W. (2016). Climate change disables coral bleaching protection on the Great Barrier Reef. *Science*, *352*, 338–342. https://doi.org/10.1126/science.aac7125

Bass, D. K., & Miller, I. R. (1996). *Crown-of-thorns starfish and coral surveys using the manta tow and scuba search techniques*. Townsville, Australia: Australian Institute of Marine Science.

Berkelmans, R., De'ath, G., Kininmonth, S., & Skirving, W. J. (2004). A comparison of the 1998 and 2002 coral bleaching events on the Great Barrier Reef: Spatial correlation, patterns, and predictions. *Coral Reefs*, *23*, 74–83. https://doi.org/10.1007/s00338-003-0353-y

Brodie, J., & Pearson, R. G. (2016). Ecosystem health of the Great Barrier Reef: Time for effective management action based on evidence. *Estuarine, Coastal and Shelf Science*, *183*, 438–451. https://doi.org/10.1016/j.ecss.2016.05.008

Broennimann, O., Treier, U., Müller-Schärer, H., Thuiller, W., & Peterson, A., Guisan, A. (2007). Evidence of climatic niche shift during biological invasion, *Ecology Letters*, *10*, 701–709.

Caley, M. J., Fisher, R., & Mengersen, K. (2014). Global species richness estimates have not converged. *Trends in Ecology & Evolution*, *29*, 187–188. https://doi.org/10.1016/j.tree.2014.02.002

Ceballos, G., Ehrlich, P. R., Barnosky, A. D., García, A., Pringle, R. M., & Palmer, T. M. (2015). Accelerated modern human–induced species losses: Entering the sixth mass extinction. *Science Advances*, *1*, e1400253. https://doi.org/10.1126/sciadv.1400253

Cheal, A. J., Macneil, M. A., Emslie, M. J., & Sweatman, H. (2017). The threat to coral reefs from more intense cyclones under climate change. *Global Change Biology*, *23*, 1511–1524. https://doi.org/10.1111/gcb.13593

Colombo-Pallotta, M. F., Rodriguez-Roman, A., & Iglesias-Prieto, R. (2010). Calcification in bleached and unbleached Montastraea faveolata: Evaluating the role of oxygen and glycerol. *Coral Reefs*, *29*, 899–907. https://doi.org/10.1007/s00338-010-0638-x

Costanza, R., de Groot, R., Sutton, P., van der Ploeg, S., Anderson, S. J., Kubiszewski, I., … Turner, R. K. (2014). Changes in the global value of ecosystem services. *Global Environmental Change*, *26*, 152–158. https://doi.org/10.1016/j.gloenvcha.2014.04.002

Cumming, G. S., Morrison, T. H., & Hughes, T. P. (2017). New directions for understanding the spatial resilience of social-ecological systems. *Ecosystems*, *20*, 649–664. https://doi.org/10.1007/s10021-016-0089-5

Darling, E. S., Alvarez-Filip, L., Oliver, T. A., Mcclanahan, T. R., & Cote, I. M. (2012). Evaluating life-history strategies of reef corals from species traits. *Ecology Letters*, *15*, 1378–1386. https://doi.org/10.1111/j.1461-0248.2012.01861.x

Davison, A. C., & Hinkley, D. V. (1997). *Bootstrap methods and their application*. Cambridge: Cambridge University Press.

Day, T., Nagel, L., Van Oppen, M. J. H., & Caley, M. J. (2008). Factors affecting the evolution of bleaching resistance in corals. *American Naturalist*, *171*, E72–E88. https://doi.org/10.1086/524956

De'ath, G. (2002). Multivariate regression trees: A new technique for modeling species-environment relationships. *Ecology*, *83*, 1105–1117.

De'ath, G., Fabricius, K. E., Sweatman, H., & Puotinen, M. (2012). The 27-year decline of coral cover on the Great Barrier Reef and its causes. *Proceedings of the National Academy of Sciences of the United States of America*, *109*, 17995–17999. https://doi.org/10.1073/pnas.1208909109

R Development Core Team. (2017). R: A language and environment for statistical computing, Vienna, Austria. ISBN 3-900051-07-0, http://www.R-project.org/. R Foundation for Statistical Computing.

Diggle, P. J., & Ribeiro, P. J. Jr (2007). *Model-based geostatistics*. New York: Springer.

Dufrêne, M., & Legendre, P. (1997). Species assemblages and indicator species: The need for a flexible asymmetrical approach. *Ecological Monographs*, *67*, 345–366. https://doi.org/10.2307/2963459

Elith, J., & Leathwick, J. R. (2009). Species distribution models: Ecological explanation and prediction across space and time. *Annual Review of Ecology Evolution and Systematics*, *40*, 677–697. https://doi.org/10.1146/annurev.ecolsys.110308.120159

Elith, J., Leathwick, J. R., & Hastie, T. (2008). A working guide to boosted regression trees. *Journal of Animal Ecology*, *77*, 802–813. https://doi.org/10.1111/j.1365-2656.2008.01390.x

Fabricius, K. E. (2005). Effects of terrestrial runoff on the ecology of corals and coral reefs: Review and synthesis. *Marine Pollution Bulletin*, *50*, 125–146. https://doi.org/10.1016/j.marpolbul.2004.11.028

Fabricius, K., Okaji, K., & De'ath, G. (2010). Three lines of evidence to link outbreaks of the crown-of-thorns seastar *Acanthaster planci* to the release of larval food limitation. *Coral Reefs*, *29*, 593–605. https://doi.org/10.1007/s00338-010-0628-z

Fisher, R., O'Leary, R. A., Low-Choy, S., Mengersen, K., Knowlton, N., Brainard, R. E., & Caley, M. J. (2015). Species richness on coral reefs and the pursuit of convergent global estimates. *Current Biology*, *25*, 500–505. https://doi.org/10.1016/j.cub.2014.12.022

Folke, C., Carpenter, S., Walker, B., Scheffer, M., Elmqvist, T., Gunderson, L., & Holling, C. S. (2004). Regime shifts, resilience, and biodiversity in ecosystem management. *Annual Review of Ecology Evolution and Systematics*, *35*, 557–581. https://doi.org/10.1146/annurev.ecolsys.35.021103.105711

Fukaya, K., Okuda, T., Nakaoka, M., Hori, M., & Noda, T. (2010). Seasonality in the strength and spatial scale of processes determining intertidal barnacle population growth. *Journal of Animal Ecology*, *79*, 1270–1279. https://doi.org/10.1111/j.1365-2656.2010.01727.x

Game, E. T., Mcdonald-Madden, E., Puotinen, M. L., & Possingham, H. P. (2008). Should we protect the strong or the weak? Risk, resilience, and the selection of marine protected areas. *Conservation Biology*, *22*, 1619–1629. https://doi.org/10.1111/j.1523-1739.2008.01037.x

Hastie, T., & Tibshirani, R. (1990). *Generalized Additive Models*. London: Chapman and Hall.

Hock, K., Wolff, N. H., Condie, S. A., Anthony, K. R. N., & Mumby, P. J. (2014). Connectivity networks reveal the risks of crown-of-thorns starfish outbreaks on the Great Barrier Reef. *Journal of Applied Ecology*, *51*, 1188–1196. https://doi.org/10.1111/1365-2664.12320

Hughes, T., Baird, A. H., Bellwood, D. R., Card, M., Connolly, S. R., Folke, C., … Lough, J. M. (2003). Climate change, human impacts, and the resilience of coral reefs. *Science*, *301*, 929–933. https://doi.org/10.1126/science.1085046

Hughes, T., Bellwood, D. R., Folke, C., Steneck, R. S., & Wilson, J. (2005). New paradigms for supporting the resilience of marine ecosystems. *Trends in Ecology and Evolution*, *20*, 380–386. https://doi.org/10.1016/j.tree.2005.03.022

Hughes, T. P., Kerry, J. T., Alvarez-Noriega, M., Álvarez-Romero, J. G., Anderson, K. D., Baird, A. H. … Bridge, T. C. (2017). Global warming and recurrent mass bleaching of corals. *Nature*, *543*, 373-+.

Hughes, T. P., NaJ, G., Jackson, J. B. C., Mumby, P. J., & Steneck, R. S. (2010). Rising to the challenge of sustaining coral reef resilience. *Trends in Ecology & Evolution*, *25*, 633–642. https://doi.org/10.1016/j.tree.2010.07.011

Hughes, T. P., Rodrigues, M. J., Bellwood, D. R., Ceccarelli, D., Hoegh-Guldberg, O., McCook, L., … Willis, B. (2007). Phase shifts, herbivory, and the resilience of coral reefs to climate change. *Current Biology*, *17*, 360–365. https://doi.org/10.1016/j.cub.2006.12.049

Jonker, M., Johns, K., & Osborne, K. (2008). *Surveys of benthic reef communities using digital photography and counts of juvenile corals. Long-term monitoring of the Great Barrier Reef standard operational procedure number 10*. Townsville, Australia: Australian Institute of Marine Science.

Knowlton, N. (2001). The future of coral reefs. *Proceedings of the National Academy of Sciences of the United States of America*, *98*, 5419–5425. https://doi.org/10.1073/pnas.091092998

Lurgi, M., Lopez, B. C., & Montoya, J. M. (2012). Novel communities from climate change. *Philosophical Transactions of the Royal Society B-Biological Sciences*, *367*, 2913–2922. https://doi.org/10.1098/rstb.2012.0238

Macneil, M. A., Mellin, C., Matthews, S., Wolff, N. H., McClanahan, T. R., Devlin, M. … Graham, N. A. (2019). Water quality mediated resilience on the Great Barrier Reef. *Nature Ecology and Evolution*, https://doi.org/10.1038/s41559-019-0832-3

Madin, J. S., Hoogenboom, M. O., & Connolly, S. R. (2012). Integrating physiological and biomechanical drivers of population growth over environmental gradients on coral reefs. *The Journal of Experimental Biology*, *215*, 968. https://doi.org/10.1242/jeb.061002

Maire, E., Cinner, J., Velez, L., Huchery, C., Mora, C., Dagata, S., … Mouillot, D. (2016). How accessible are coral reefs to people? A global assessment based on travel time. *Ecology Letters*, *19*, 351–360. https://doi.org/10.1111/ele.12577

Matthews, S., Mellin, C., Macneil, M. A., Heron, S., Puotinen, M. L., & Pratchett, M. (2019). Disturbance and environment data for the Great Barrier Reef: A comprehensive characterisation of the abiotic environment and disturbances regimes; 1985–2016. *Ecology*, https://doi.org/10.1002/ecy.2574

Medley, K. A. (2010). Niche shifts during the global invasion of the Asian tiger mosquito, Aedes albopictus Skuse (Culicidae), revealed by reciprocal distribution models. *Global Ecology and Biogeography*, *19*, 122–133.

Mellin, C. (2015). Abiotic surrogates in support of marine biodiversity conservation. In D. B. Lindenmayer, P. Barton, & Pierson, J. (Eds.), *Indicators and Surrogates of Biodiversity and Environmental Change* (216 p). Melbourne, Australia: CSIRO Publishing.

Mellin, C., Andrefouet, S., Kulbicki, M., Dalleau, M., & Vigliola, L. (2009). Remote sensing and fish-habitat relationships in coral reef ecosystems: Review and pathways for systematic multi-scale hierarchical research. *Marine Pollution Bulletin*, *58*, 11–19.

Mellin, C., Bradshaw, C. J. A., Meekan, M. G., & Caley, M. J. (2010). Environmental and spatial predictors of species richness and abundance in coral reef fishes. *Global Ecology and Biogeography*, *19*, 212–222.

Mellin, C., Huchery, C., Caley, M. J., Meekan, M. G., & Bradshaw, C. J. A. (2010). Reef size and isolation determine the temporal stability of coral reef fish populations. *Ecology*, *91*, 3138–3145.

Mellin, C., Macneil, M. A., Cheal, A. J., Emslie, M. J., & Caley, M. J. (2016). Marine protected areas increase resilience among coral reef communities. *Ecology Letters*, *19*, 629–637. https://doi.org/10.1111/ele.12598

Miller, I., & Müller, R. (1999). Validity and reproducibility of benthic cover estimates made during broadscale surveys of coral reefs by manta tow. *Coral Reefs*, *18*, 353–356. https://doi.org/10.1007/s003380050212

Mumby, P. J., & Anthony, K. R. N. (2015). Resilience metrics to inform ecosystem management under global change with application to coral reefs. *Methods in Ecology and Evolution*, *6*, 1088–1096. https://doi.org/10.1111/2041-210X.12380

Mumby, P. J., Chollett, I., Bozec, Y.-M., & Wolff, N. H. (2014). Ecological resilience, robustness and vulnerability: How do these concepts benefit ecosystem management? *Current Opinion in Environmental Sustainability*, *7*, 22–27.

Mumby, P. J., Elliott, I. A., Eakin, C. M., Skirving, W., Paris, C. B., Edwards, H. J., … Stevens, J. R. (2011). Reserve design for uncertain responses of coral reefs to climate change. *Ecology Letters*, *14*, 132–140. https://doi.org/10.1111/j.1461-0248.2010.01562.x

Norton, J. (2015). An introduction to sensitivity assessment of simulation models. *Environmental Modelling & Software*, *69*, 166–174. https://doi.org/10.1016/j.envsoft.2015.03.020

Ortiz, J. C., Wolff, N. H., Anthony, K. R. N., Devlin, M., Lewis, S., & Mumby, P. J. (2018). Impaired recovery of the Great Barrier Reef under cumulative stress. Science. *Advances*, *4*, eaar6127. https://doi.org/10.1126/sciadv.aar6127

Osborne, K., Dolman, A. M., Burgess, S. C., & Johns, K. A. (2011). Disturbance and the dynamics of coral cover on the Great Barrier Reef (1995–2009). *PLoS ONE*, *6*, 1–10. https://doi.org/10.1371/journal.pone.0017516

Osborne, K., Thompson, A. A., Cheal, A. J., Emslie, M. J., Johns, K. A., Jonker, M. J., … Sweatman, H. P. A. (2017). Delayed coral recovery in a warming ocean. *Global Change Biology*, *23*, 3869–3881. https://doi.org/10.1111/gcb.13707

Pearson, R. G., Stanton, J. C., Shoemaker, K. T., Aiello-Lammens, M. E., Ersts, P. J., Horning, N. … Akçakaya, H. R. (2014). Life history and spatial traits predict extinction risk due to climate change. *Nature Clim. Change*, *4*, 217–221.

Petus, C., Da Silva, E. T., Devlin, M., Wenger, A. S., & Alvarez-Romero, J. G. (2014). Using MODIS data for mapping of water types within river plumes in the Great Barrier Reef, Australia: Towards the production of river plume risk maps for reef and seagrass ecosystems. *Journal of Environmental Management*, *137*, 163–177.

Pratchett, M., Anderson, K., Hoogenboom, M., Widman, E., Baird, A. H., Pandolfi, J. M. … Lough, J. M. (2015). Spatial, temporal and taxonomic variation in coral growth - implications for the structure and function of coral reef ecosystems. *Oceanography and Marine Biology: an Annual Review*, *53*, 215–295.

Pratchett, M. S., Caballes, C. F., Rivera-Posada, J. A., & Sweatman, H. P. (2014). Limits to understanding and managing outbreaks of crown-of-thorns starfish (*Acanthaster* Spp.). Oceanography and Marine. *Biology: an Annual Review*, *52*, *52*, 133–199.

Puotinen, M., Maynard, J. A., Beeden, R., Radford, B., & Williams, G. J. (2016). A robust operational model for predicting where tropical cyclone waves damage coral reefs. *Scientific Reports*, *6*, 26009. https://doi.org/10.1038/srep26009

Roland Pitcher, C., Lawton, P., Ellis, N., Smith, S. J., Incze, L. S., Wei, C.-L., … Snelgrove, P. V. R. (2012). Exploring the role of environmental variables in shaping patterns of seabed biodiversity composition in regional-scale ecosystems. *Journal of Applied Ecology*, *49*, 670–679. https://doi.org/10.1111/j.1365-2664.2012.02148.x

Salvatier, J., Wiecki, T. V., & Fonnesbeck, C. (2016). Probabilistic programming in Python using PyMC3. *PeerJ Computer Science*, *2*, e55. https://doi.org/10.7717/peerj-cs.55

Sutcliffe, P., Mellin, C., Pitcher, C., Possingham, H., & Caley, M. (2014). Regional-scale patterns and predictors of species richness and abundance across twelve major tropical inter-reef taxa. *Ecography*, *37*, 162–171. https://doi.org/10.1111/j.1600-0587.2013.00102.x

Sweatman, H., Cheal, A., Coleman, G., Emslie, M., Johns, K., Jonker, M., … Osborne, K. (2008). *Long-term monitoring of the Great Barrier Reef. Status Report no8*. Townsville, Australia: Australian Institute of Marine Science.

Thompson, A., Costello, P., Davidson, J., Logan, M., Gunn, K., & Schaffelke, B. (2016). *Marine monitoring program: Annual report for inshore coral reef monitoring*. Townsville, Australian Institute of Marine Science: Report for the Great Barrier Reef Marine Park Authority.

Thurber, R. L. V., Burkepile, D. E., Fuchs, C., Shantz, A. A., Mcminds, R., & Zaneveld, J. R. (2014). Chronic nutrient enrichment increases prevalence and severity of coral disease and bleaching. *Global Change Biology*, *20*, 544–554. https://doi.org/10.1111/gcb.12450

Uthicke, S., Logan, M., Liddy, M., Francis, D., Hardy, N., & Lamare, M. (2015). Climate change as an unexpected co-factor promoting coral eating seastar (Acanthaster planci) outbreaks. *Scientific Reports*, 5.

Van Hooidonk, R., Maynard, J. A., & Planes, S. (2013). Temporary refugia for coral reefs in a warming world. *Nature Climate Change*, *3*, 508–511. https://doi.org/10.1038/nclimate1829

Van Hooidonk, R., Maynard, J., Tamelander, J., Gove, J., Ahmadia, G., Raymundo, L., … Planes, S. (2016). Local-scale projections of coral reef futures and implications of the Paris Agreement. *Scientific Reports*, *6*.

van Oppen, M. J. H., Gates, R. D., Blackall, L. L., Cantin, N., Chakravarti, L. J., Chan, W. Y., … Putnam, H. M. (2017). Shifting paradigms in restoration of the world's coral reefs. *Global Change Biology*, *23*, 3437–3448. https://doi.org/10.1111/gcb.13647

Vercelloni, J., Caley, M. J., & Mengersen, K. (2017). Crown-of-thorns starfish undermine the resilience of coral populations on the Great Barrier Reef. *Global Ecology and Biogeography*, *26*, 846–853. https://doi.org/10.1111/geb.12590

Walsh, K. J. E., McBride, J. L., Klotzbach, P. J., Balachandran, S., Camargo, S. J., Holland, G., … Sugi, M. (2016). Tropical cyclones and climate change. *Wiley Interdisciplinary Reviews: Climate Change*, *7*, 65–89. https://doi.org/10.1002/wcc.371

Wenger, A. S., Williamson, D. H., Da Silva, E. T., Ceccarelli, D. M., Browne, N. K., Petus, C., & Devlin, M. J. (2016). Effects of reduced water quality on coral reefs in and out of no-take marine reserves. *Conservation Biology*, *30*, 142–153. https://doi.org/10.1111/cobi.12576

Wolff, N. H., Mumby, P. J., Devlin, M., & Anthony, K. R. N. (2018). Vulnerability of the Great Barrier Reef to climate change and local pressures. *Global Change Biology*, *24*, 1978–1991. https://doi.org/10.1111/gcb.14043

Yates, K. L., Bouchet, P. J., Caley, M. J., Mengersen, K., Randin, C. F., Parnell, S., … Sequeira, A. M. M. (2018). Outstanding challenges in the transferability of ecological models. *Trends in Ecology & Evolution*, *33*, 790–802. https://doi.org/10.1016/j.tree.2018.08.001

SUPPORTING INFORMATION

Additional supporting information may be found online in the Supporting Information section at the end of the article.

How to cite this article: Mellin C, Matthews S, Anthony KRN, et al. Spatial resilience of the Great Barrier Reef under cumulative disturbance impacts. *Glob Change Biol*. 2019;25:2431–2445. https://doi.org/10.1111/gcb.14625